JOURNAL OF MATERIALS SCIENCE **36** (2001) 1363–1371

Identification of the nitrides formed during the annealing of a low-carbon low-aluminium steel

V. MASSARDIER, L. VORON, C. ESNOUF, J. MERLIN
Groupe d'Etudes de Métallurgie Physique et de Physique des Matériaux, UMR CNRS 5510, INSA Lyon, Bât. 502, F-69621 Villeurbanne Cedex, France
E-mail: veronique.massardier@insa-lyon.fr

The precipitation of a low carbon low aluminium steel with a sub-stoichiometric [Al]/[N] atomic ratio was investigated during an annealing at 600°C by Transmission Electron Microscopy (TEM) and chemical analyses by X-ray Energy Dispersive Spectroscopy (EDX) on thin foils and carbon extraction replicas. These studies showed that in this steel, the precipitates which form have a platelet-like morphology associated with a cubic structure (with $a = 0.412 \pm 0.005$ nm) and the following orientation relationship with iron: $(001)_p$ // $(001)_{Fe}$ and $[110]_p$ // $[010]_{Fe}$. The EDX microanalyses of these precipitates revealed that they contain, in addition to aluminium and nitrogen, chromium and/or manganese. It was suggested that in the early stages of annealing, the initial precipitates are of CrN or (Cr,Mn)N type. During a prolonged annealing, they serve as nucleation sites for the final precipitates of (Al,Cr)N and (Al,Cr,Mn)N type.

1. Introduction

The texture of recrystallization of cold-rolled aluminium-killed steels is greatly controlled by the interactions which may occur, during the annealing, between the recrystallization and the precipitation of aluminium nitrides (AlN) [1–6]. In particular, the works of Meyzaud *et al.* [4] showed that the interaction between recovery, recrystallyzation and precipitation of AlN is dependent both on the annealing temperature and on the heating rate. In the case of a batch annealing (where the annealing temperature is of the order of 600°C and the heating rate is between 20 and 200 $K \cdot h^{-1}$), the AlN precipitation interacts with the recrystallization, which leads to the formation of a {111} texture. This texture is generally recognised as being responsible for the good drawability of cold-rolled and annealed Al-killed steels and seems to result from an inhibition of the growth of the sub-grains by the AlN precipitation, followed then by the growth of sub-grains of {111} type after coarsening of the AlN particles [3–6].

However, it has to be noted that the evidence of the formation of the AlN precipitates during the recrystallization annealing was not always clearly established. Indeed, some authors [1–3], using direct observations of thin foils or of carbon extraction replicas, did not detect the AlN particles supposed to form during the annealing treatment. As a consequence, they supposed that the effective precipitates were in a state of pre-precipitation clusters of AlN.

Furthermore, it was observed by Merlin *et al.* [7], on a steel with a sub-stoichiometric [Al]/[N] atomic ratio, a complete elimination of nitrogen from the solid solution. As a consequence, the precipitation of stoichiometric AlN is unlikely in this steel, since its aluminium content can not be responsible for the consumption of all the nitrogen present in solid solution. This can be attributed to the presence in the nitrides of elements other than aluminium and/or to an adsorption of nitrogen at the AlN/α-Fe interface, as was suggested by Biglari *et al.* [8].

The aim of this work is thus to clearly identify the nitrides which form during the annealing of a low-carbon low-aluminium steel, with a sub-stoichiometry in aluminium, both from a chemical and structural point of view, using Conventional and High-Resolution Transmission Electron Microscopy (CTEM and HRTEM) combined with chemical analyses by X-ray Energy Dispersive Spectroscopy (EDX).

2. Material and experimental procedure

2.1. Material

The material investigated is a low-carbon low-aluminium steel having a microstructure characterised by equiaxed grains. Its chemical composition, expressed in weight percentage, is the following: 56×10^{-3} wt.% C, 11×10^{-3} wt.% N, 14×10^{-3} wt.% Al, 12×10^{-3} wt.% Cr and about 300×10^{-3} wt.% Mn. With regard to the composition of the steel, the maximum amount of stoichiometric AlN, which can precipitate, is 23×10^{-3} %, leading theoretically to about 5×10^{-3} % of nitrogen left in solid solution at the end of the precipitation. A previous work, performed on this steel and based on internal friction and thermoelectric power measurements [7], showed that the initial nitrogen content in solid solution is of the order of 10×10^{-3} wt. % and that this nitrogen begins to precipitate after 1 h of isothermal annealing at 600°C and has

completely disappeared from the solid solution after about 250 h at 600°C, supporting the hypothesis of the formation of nitrides other than stoichiometric AlN. As a consequence, this steel was studied after different annealing times at 600°C ranging between 1 h and 280 h (1 h, 6 h, 38 h and 280 h). The samples were isothermally treated under vacuum, so as to avoid oxidation.

2.2. Transmission electron microscopy (TEM) observations

The TEM investigations on the studied steel were conducted on a field-emission gun JEOL 2010F microscope operating at 200 kV and equipped with a slow-scan CCD camera (1 K × 1 K, Gatan) and with an Energy Dispersive X-ray (EDX) analyser having an ultra-thin window and a Link Isis analytical system (Oxford Instruments).

To characterise the morphology and the size of the precipitates formed during the different annealings, conventional transmission electron microscopy observations were carried out both on thin foils and on carbon extraction replicas of the studied steel. They were prepared using respectively conventional electropolishing and a standard technique.

2.3. Determination of the chemical composition of the precipitates

Nanometric probe analyses were conducted on the precipitates present on the replicas, in order to determine their chemical composition. From an experimental point of view, the analyses were performed on several precipitates present on the replicas: around 40 precipitates were analysed in each state investigated, in order to obtain average values on the chemical composition of the precipitates. From the obtained spectra, the mean atomic ratios of the elements were calculated taking into account an absorption correction.

For the analysis of the obtained EDX spectra, it was necessary to identify the peaks due to the precipitates and those due to their environment or to artefacts linked to the method of preparation of the replicas.

On all the spectra, carbon and copper peaks were always detected. They were attributed respectively to the carbon of the replicas and to the copper grids on which the replicas are put. As a consequence, these two elements could not be quantified.

Furthermore, the presence of silicon and oxygen peaks was observed very frequently. These peaks were attributed to a contamination of the replicas during the carbon deposition by evaporation. The silicon could come from the diffusion pump oil used and the oxygen is probably due to the oxidation of the silicon. The absence of silicon and oxygen in the precipitates was confirmed by comparing spectra performed on the precipitates and on the background located in the vicinity of the precipitates.

Lastly, some EDX spectra revealed the presence of iron peaks probably due to an insufficient replica washing.

It is also important to note that the height and width of the carbon peak, which is located in the vicinity of the nitrogen peak, did not allow the nitrogen content of the nitrides to be quantified accurately. Indeed, as can be seen in Fig. 5a, the carbon and nitrogen peaks overlap, which makes the quantification of nitrogen very imprecise.

2.4. Determination of the structure of the precipitates

In order to identify the structure of the precipitates, selected area electron diffraction (SAED) patterns and high resolution transmission electron microscopy images were obtained from the precipitates. Numerical fast-Fourier transforms of the HRTEM images recorded with the on-line slow-scan camera were obtained, in order to obtain the corresponding numerical diffractograms.

3. Results

3.1. Conventional TEM observations

3.1.1. Thin foils

The TEM observations of the samples annealed for 1 h and 6 h at 600°C did not show the presence of precipitates formed during the annealing. After 1 h, no precipitates were detected, since they did not have enough time to form. After 6 h, it is likely that the precipitates were too small to be detected.

In contrast, the TEM observations of the samples annealed for 38 and 280 h at 600°C clearly indicated the presence of numerous precipitates present inside the grains. In fact, the precipitates are not apparent but they can be detected, as they give rise to a contrast arising from a strain field around them. This kind of contrast was studied by Ashby and Brown [9] and is clearly visible in Fig. 1a and b. It generally indicates a distorsion of the matrix around a coherent precipitate having a small misfit. In the case of Fig. 1a, the lines of no contrast associated with each precipitate are perpendicular to the diffracting vector **g**, which is in a ⟨110⟩ direction of the ferrite. In Fig. 1a, the contrast around each precipitate is thus essentially due to the deformation of the iron lattice induced by the presence of coherent precipitates. However, it has to be noted that in the case of Fig. 1b where the zone axis is close to a $\langle 100 \rangle_{Fe}$ direction, the lines of no contrast are not perpendicular to the diffracting vector and are parallel to the ⟨100⟩ directions of the iron matrix. This indicates that the contrast observed in Fig. 1b is mainly due to the geometry of the precipitates. From these observations, it is possible to conclude that the nitrides formed during the annealing at 600°C are platelets growing on the {100} habit planes of the ferrite. Three different spatial orientations are thus expected for these platelets in the iron matrix. When viewed with their habit plane parallel to the electron beam, these platelets appear as lines oriented along the ⟨100⟩ directions of the ferrite. Depending on the imaging conditions, one or two populations of precipitates oriented at 90° from each other can be observed.

3.1.2. Carbon extraction replicas

The CTEM observations carried out on the precipitates present on the replicas showed that after 1 h at 600°C,

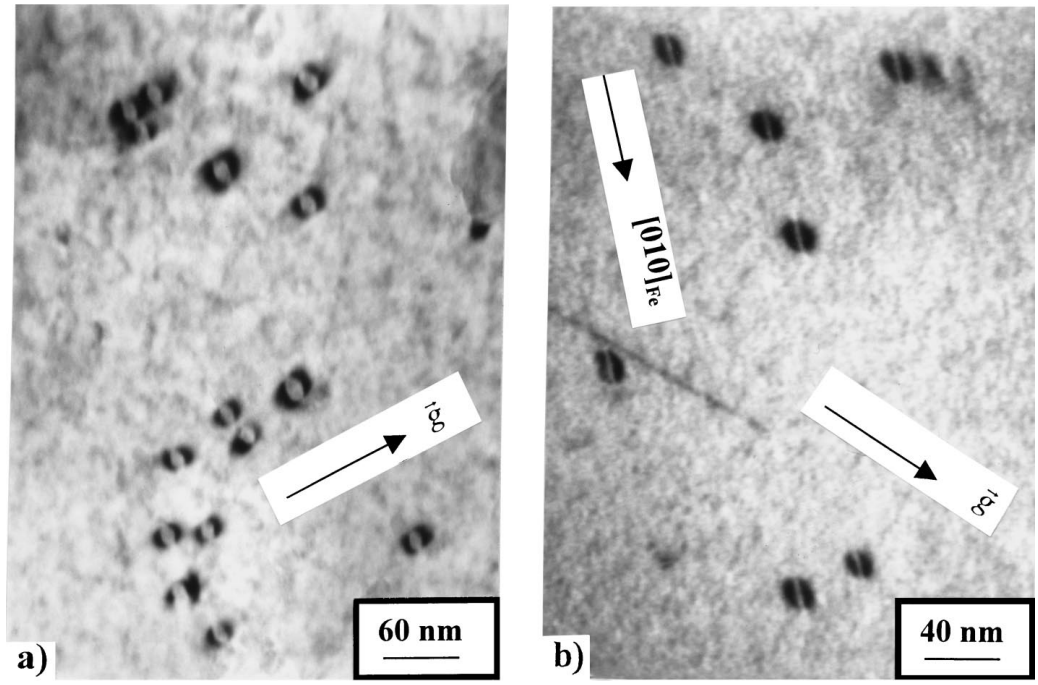

Figure 1 TEM micrographs of the investigated steel annealed for 280 hrs at 600°C showing: (a) the deformation contrast induced by the precipitates and (b) a contrast due mainly to the geometry of the nitrides. In each micrograph, the diffracting vector is parallel to a ⟨110⟩ direction of the ferrite. In Fig. 1a, this vector is perpendicular to the lines of no contrast associated with each precipitate, while in Fig. 1b, it is not perpendicular to the lines of no contrast which are aligned along the ⟨100⟩ directions of iron.

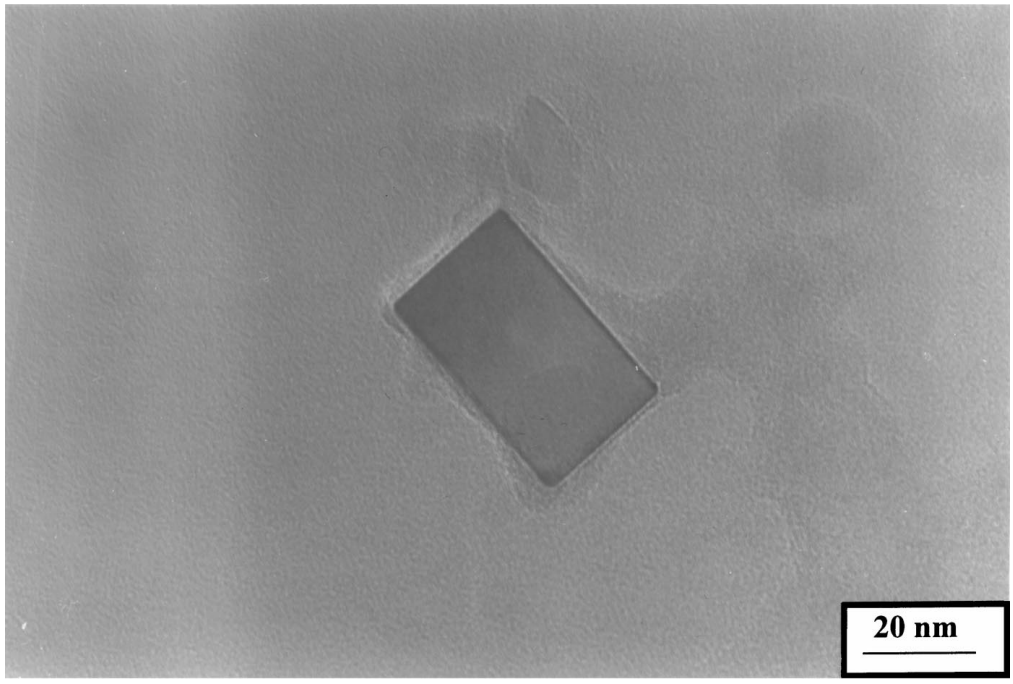

Figure 2 TEM micrograph of a TiN precipitate.

the only precipitates which are detected (in addition to the precipitates of cementite) are angular particles, the size of which is of the order of 50 nm and the geometry of which is typical of that of the titanium nitride (Fig. 2). This was confirmed by the EDX microanalysis of these precipitates. In fact, these precipitates are very stable and did not form during the annealing at 600°C but at a higher temperature during the processing of the steel.

After 6 h at 600°C, the CTEM observations showed the presence of a few small particles, having a size less than 10 nm and without a particular shape. After 38 and 280 h at 600°C, it was noted that these particles are much more numerous and have increased in size.

Fig. 3 shows different CTEM micrographs of these particles extracted from the sample annealed for 280 h at 600°C. Owing to the fact that the precipitates have different orientations on the replicas, these micrographs reveal different morphologies (in particular, squares or rectangles which are more or less elongated). When viewed with their large face perpendicular to the electron beam (as in the case of Fig. 3b), the platelet-like morphology of the particles is clearly visible. As a

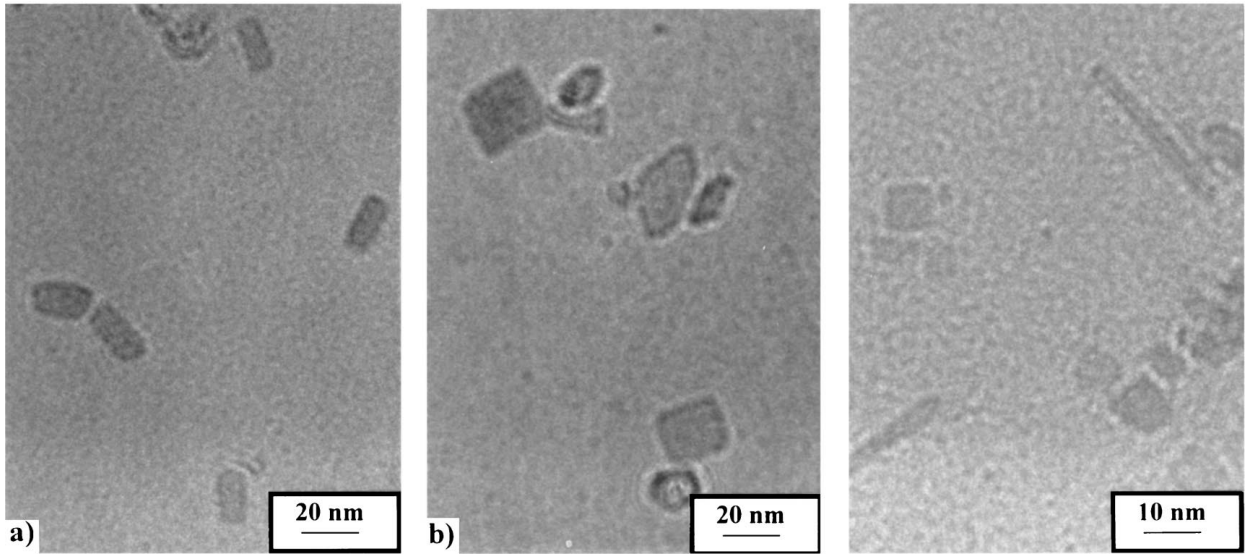

Figure 3 TEM micrographs showing the different morphologies of the precipitates present on the replicas of the sample annealed for 280 hrs at 600°C.

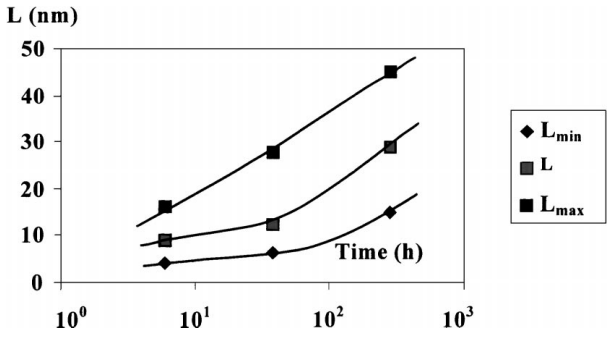

Figure 4 Evolution of the mean length and of the minimum and maximum length of the precipitates with the annealing time at 600°C.

conclusion, all these observations tend to support the hypothesis that the precipitates formed during the annealing grow in the iron matrix in the form of platelets.

The evolution of the size (in fact, the mean, maximum and minimum length) of the precipitates with the annealing time is represented in Fig. 4. It appears clearly that the size of the precipitates increases regularly with increasing the annealing time.

3.2. EDX analyses: chemical composition of the precipitates

The EDX analyses performed showed that the precipitates formed during the annealing at 600°C are not aluminium nitrides but rather complex compounds containing, in addition to aluminium and nitrogen, chromium (precipitates of (Al,Cr)N type) or manganese (precipitates of (Al,Mn)N type) or both chromium and manganese (precipitates of (Al,Cr,Mn)N type). It has to be noted that this last type of precipitates was found to be largely predominant, while the precipitates of (Al,Mn)N type were not observed very frequently and will not be taken into account hereafter.

Fig. 5b to d show examples of EDX spectra obtained on the different types of precipitates mentioned above. An evolution of the relative height of the peaks with the annealing time was observed, indicating an evolution of the chemical composition of the precipitates.

TABLE I Chemical composition of the nitrides formed after different isothermal annealings performed at 600°C. The nitrogen content of the precipitates was not taken into account

Annealing time at 600°C	Type of precipitate	Atomic percentage		
		Al	Cr	Mn
6 h	(Al,Cr,Mn)N	37 ± 8	44 ± 8	19 ± 6
	(Al,Cr)N	44 ± 8	56 ± 8	
38 h	(Al,Cr,Mn)N	77 ± 8	17 ± 8	6 ± 3
	(Al,Cr)N	84 ± 6	16 ± 6	
280 h	(Al,Cr,Mn)N	76 ± 4	16 ± 4	8 ± 2
	(Al,Cr)N	79 ± 4	21 ± 4	

Table I gives the aluminium, chromium and manganese content of the studied precipitates in atomic percentage for different annealing times at 600°C, while Fig. 6 represents the evolution of the mean [Al]/[Cr], [Al]/[Mn], [Al]/([Cr] + [Mn]) and [Cr]/[Mn] atomic ratios of the precipitates of (Al,Cr,Mn)N type with the annealing time.

For this last type of precipitate, it appears that: (i) the [Cr]/[Mn] atomic ratio does not evolve between the three states of annealing considered (6, 38 and 280 h), (ii) the [Al]/[Cr], [Al]/[Mn] and [Al]/([Cr] + [Mn]) atomic ratios increase between 6 h and 38 h, (iii) the proportions in Al, Cr, Mn are quite similar for the states annealed for 38 h and 280 h at 600°C. As a conclusion, even after 6 h at 600°C, the precipitates formed have reached their equilibrium [Cr]/[Mn] atomic ratio. Then, these precipitates enrich in aluminium (from 6 h to 38 h), until they reach their equilibrium composition.

As far as the precipitates of (Al,Cr)N type are concerned, they have the same type of behaviour. Initially rich in chromium, these precipitates have their aluminium content which increases between 6 h and 38 h of annealing at 600°C. Then, no chemical evolution of their composition is detected between 38 h and 280 h.

3.3. Identification of the crystallographic structure of the nitrides

In order to identify the structure of the nitrides formed in the steel annealed for 280 h at 600°C, diffraction

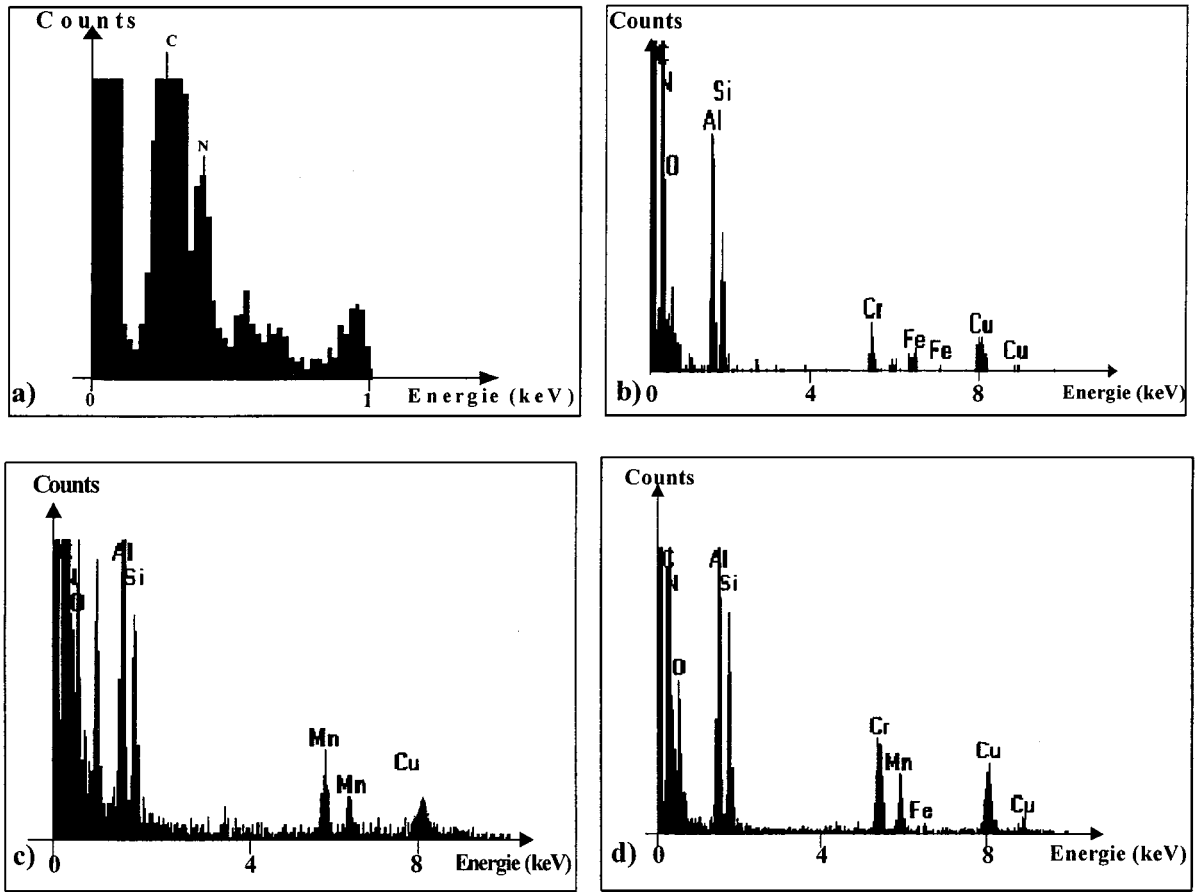

Figure 5 (a) EDS spectrum showing the overlapping of the carbon and nitrogen peaks, (b), (c) and (d) Examples of EDS spectra obtained on the different types of precipitates observed.

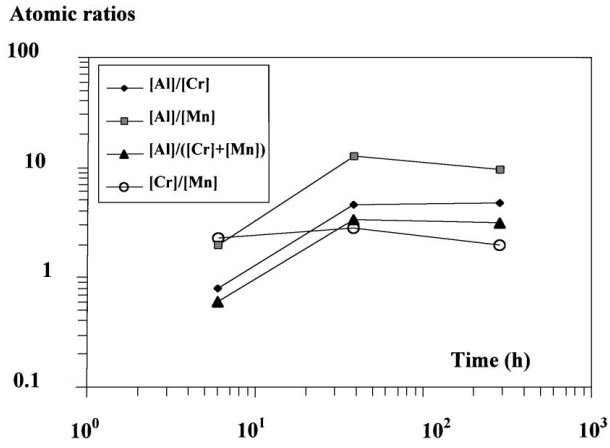

Figure 6 Evolution of the [Al]/[Cr], [Al]/[Mn], [Al]/([Cr] + [Mn]) and [Cr]/[Mn] atomic ratios with the annealing time at 600°C.

patterns of individual precipitates present on the corresponding replicas were obtained. The diffraction patterns were obtained either directly by selected-area electron diffraction or by fast-Fourier transforms of HRTEM images.

Fig. 7 shows a platelet of (Al,Cr,Mn)N type viewed with its large face perpendicular to the electron beam and the corresponding SAED pattern. This pattern, which presents a 4mm symmetry, can be interpreted as being due a cubic lattice observed along a zone axis of ⟨100⟩ type.

This interpretation was confirmed by the analysis of diffraction pattern of the nitride of (Al,Cr,Mn) type, shown in Fig. 8a and observed with its habit plane parallel to the electron beam. Fig. 8b and c show respectively the corresponding Fourier filtered image (obtained from the HRTEM micrograph of a detail of the precipitate) and the numerical diffractogram of the precipitate. This diffractogram can unambiguously be interpreted as being due to a f.c.c. lattice viewed along a ⟨110⟩ zone axis.

Using this result, the SAED pattern of Fig. 7 could be indexed on the basis of a f.c.c. lattice. This pattern indicates that the large face of the platelets is parallel to a {100} plane of the f.c.c. lattice. Furthermore, as the TEM observations of the nitrides present in the iron matrix (Section 3.1.1.) or on the carbon replicas (Section 3.1.2) led us to the conclusion that these nitrides are platelets growing on the {100} habit planes of the ferrite, this supports that the studied precipitates and the parent iron matrix are oriented such that:

$$(001)_p // (001)_{Fe}$$

3.4. Determination of the orientation relationship of the nitrides with the iron matrix and of their lattice parameter

In order to completely determine the orientation relationship of the nitrides with the iron matrix, a further HRTEM investigation was performed on nitrides present on a thin foil of the steel treated for 280 h at 600°C. Fig. 9a shows the numerical diffractogram of a nitride having its habit plane parallel to the electron beam, this one being aligned along a $\langle 100 \rangle_{Fe}$ direction

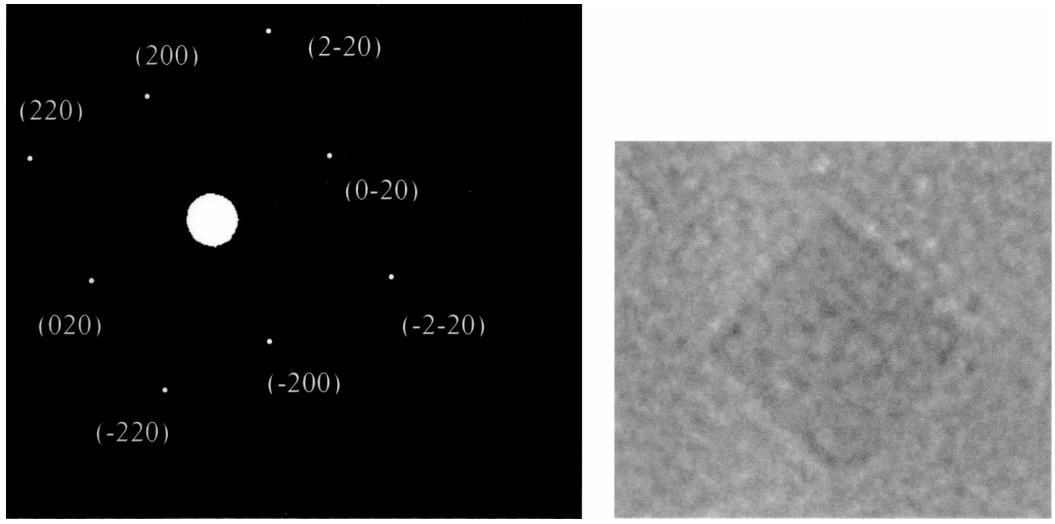

Figure 7 TEM micrograph and SAED pattern of a platelet of (Al,Cr,Mn)N type viewed with its large face perpendicular to the electron beam.

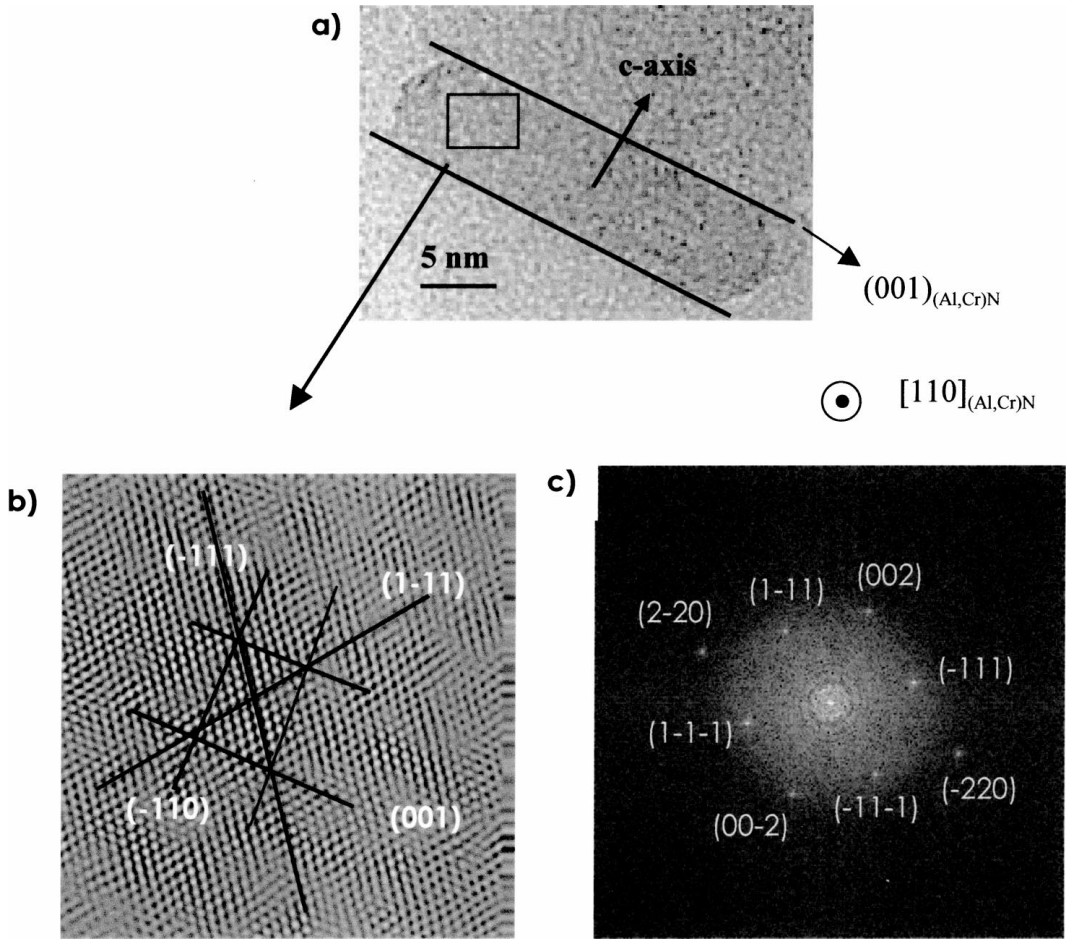

Figure 8 Precipitate of (Al,Cr,Mn) type viewed with its large face parallel to the electron beam: (a) general view of the precipitate, (b) Fourier-filtered image of the precipitate and (c) associated numerical diffractogram.

of the ferrite. In addition to the spots due to the ferrite, spots due to the nitride are clearly visible. The scheme of Fig. 9b is the representation of the numerical diffractogram of Fig. 9a and shows that it is the superposition of the diffraction pattern of the ferrite viewed along a ⟨100⟩ direction and that of the studied nitride observed along a ⟨110⟩ direction of a f.c.c. lattice (as in Fig. 8). Furthermore, the relative position of the spots due to the ferrite and of those due to the nitride clearly provide evidence (as was already suggested in Section 3.3.) that the (001) planes of the ferrite are parallel to the (001) planes of the precipitate.

From all these information, one can conclude that the crystallographic relations between the studied nitrides and the iron matrix are as follows:

$$[110]_p // [010]_{Fe} \quad \text{and} \quad (001)_p // (001)_{Fe}$$

This orientation relationship is commonly called Bain orientation relationship [10] and was already reported

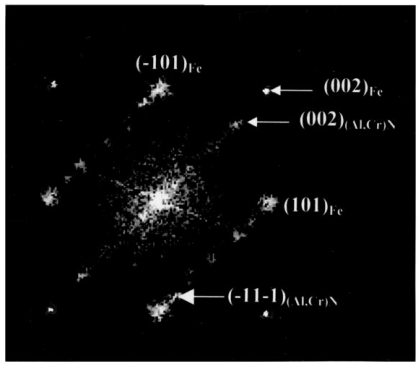

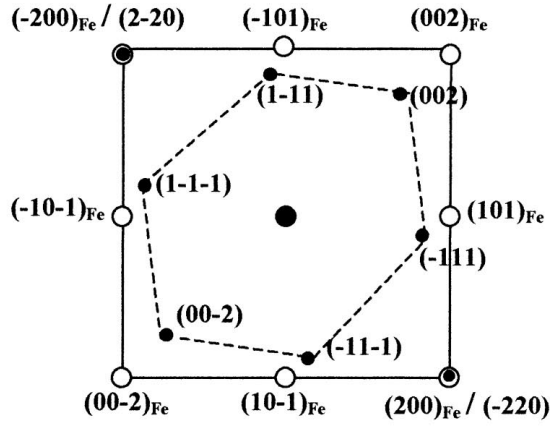

$[110]_{(Al,Cr)N}$ // $[010]_{Fe}$

(a) (b)

Figure 9 (a) Numerical diffractogram of a nitride of (Al,Cr)N type viewed with its habit plane parallel to the electrom beam (b) Scheme giving the crystallographic relations between the studied nitrides and the iron matrix. ● nitride ○ ferrite.

by other authors [11] for the cubic (rock salt) AlN in ferrite.

Furthermore, the diffractrogram of Fig. 9a allowed us to calculate the lattice parameter of the studied nitrides, after calibration of the distances measured on the diffractogram using the (002) spot of the ferrite. The parameter of the f.c.c. lattice of the nitrides was assessed using their (002) reflection. In these conditions, the lattice parameter a of the nitrides was found to be of the order of 0.412 ± 0.005 nm.

This result was also confirmed by a study of the Debye-Scherrer rings obtained from the diffraction of several precipitates. After indexation of these rings, assuming a f.c.c. lattice, the same value of a was found.

It has to be noted that this parameter is very similar to that of the cubic (rock salt) structure of AlN ($a \approx 0.410-0.417$ nm) [12] and to that of the cubic (rock salt) structure of CrN ($a = 0.414$ nm) [13].

4. Discussion

4.1. General considerations on the formation of nitrides in steels

The formation of nitrides, such as VN, TiN and CrN, in steels was clearly established by different authors [14–20]. These nitrides form in the ferrite without difficulty. They all have a rock salt (NaCl type) cubic structure and grow in the ferrite according to a Bain orientation relationship.

In contrast, according to different authors [8, 21–23], the nucleation of aluminium nitride in steel is expected to be rather difficult, unless precipitation is enhanced by mechanical treatments (such as cold-rolling). Furthermore, the aluminium nitride appears to have two different structures in ferrous metals: (i) a hexagonal wurtzite crystal structure with $a = 0.311$ nm and $c = 0.4978$ nm, as was shown for example by Wilson *et al.* [21] and (ii) a cubic structure of NaCl type with a ranging between 0.4045 nm and 0.417 nm depending on the authors [12, 24–26]. In the case where cubic AlN precipitates form, it is observed [11] that they have a platelet-like morphology and are oriented with respect to the iron matrix according to a Bain orientation relationship.

4.2. Interpretation of the present observations

The present investigations showed that the precipitates formed during the annealing of the studied steel were different from aluminium nitrides (with the AlN stoichiometry) and were complex compounds containing, in addition to nitrogen and aluminium, chromium and/or manganese. It was established that these precipitates have a f.c.c. lattice and grow in the iron matrix in the form of platelets having a $\{100\}_{Fe}$ habit plane. They are oriented in the ferrite according to the following orientation relationship:

$$(001)_p // (001)_{Fe} \quad \text{and} \quad [110]_p // [010]_{Fe}$$

It seems now interesting to discuss the mechanisms of formation of the precipitates of (Al,Cr)N and (Al,Cr,Mn)N type found in this steel.

From the above considerations, one can suggest that the initial precipitates formed in the early stages of the annealing at 600°C are probably of CrN or (Cr,Mn)N type. Several reasons tend to support this hypothesis:

(i) the formation of semi-coherent platelets of CrN type and having a cubic structure was already observed in steels treated at temperatures close to 600°C [19, 20]. These platelets were found to grow in the iron matrix according to the scheme given in Fig. 10. The (001) planes are the coherency planes. The CrN cube develops on the four diagonals of the (001) planes of iron. The coherency can be kept, since these diagonals have a length equal to 0.404 nm, which is very close to the lattice parameter of CrN ($a_{CrN} = 0.414$ nm).

(ii) the curves of Fig. 6 reveal that the initial precipitates are essentially chromium-rich. Then, they gradually enrich in aluminium, until they reach their equilibrium composition.

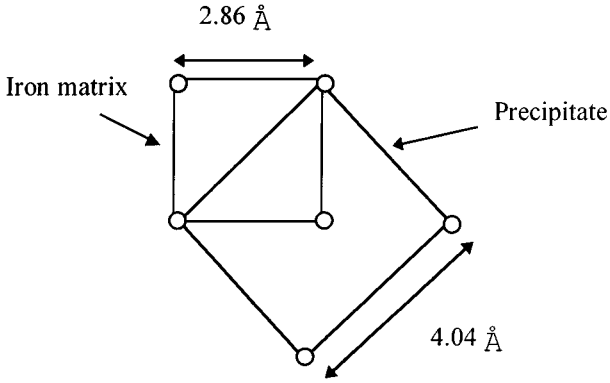

Figure 10 Scheme giving the crystallographic relations between a semi-coherent CrN platelet and the iron matrix.

(iii) the formation of AlN particles, in the early stages of the annealing, is expected to be difficult in the investigated steel, as it is characterised by a sub- stoichiometry in aluminium.

After the formation of CrN or (Cr,Mn)N precipitates, one can expect that these precipitates serve as nucleation sites for the final precipitates and enrich in aluminium and nitrogen, to give cubic (Al,Cr)N and (Al,Cr,Mn)N particles.

Lastly, from the present results, it is possible to explain why the nitrogen present in the studied steel can completely disappear from the solid solution, although it has a sub-stoichiometric [Al]/[N] atomic ratio. Considering the chemical composition of the investigated steel, its initial nitrogen and aluminium content in solid solution, expressed here in atomic percentage, is respectively 40×10^{-3} at.% and 28×10^{-3} at.%. If it is assumed that stoichiometric AlN particles form during the annealing, there is a lack of 12×10^{-3} at.% of aluminium to totally consume the nitrogen in solid solution. In fact, this lack can be compensated by 12×10^{-3} at. % of chromium and manganese, which leads to precipitates with about 70% Al and 30% (Cr + Mn). This result is in good agreement with the experimental results given by the EDX microanalyses for the long annealing times.

It should be noted that the explanation presented above is likely to account for the consumption of all the nitrogen initially in solid solution and for the chemical analyses obtained on the nitrides, without referring to the adsorption of nitrogen at the nitride/α-Fe interfaces [8]. However, as the present investigations did not allow the nitrogen content of the precipitates to be determined, it is not possible to know whether such an adsorption of nitrogen occurs in the case of the investigated nitrides.

5. Conclusion

The present work showed that:

1. In a steel with a sub-stoichiometric [Al]/[N] atomic ratio and containing, in addition to aluminium, elements such as chromium and manganese, the formation of aluminium nitrides of hexagonal or cubic structure is not observed during an annealing performed at 600°C.

2. The precipitates formed are of (Al,Cr,Mn)N and (Al,Cr)N type. They have a cubic structure with a lattice parameter $a = 0.412 \pm 0.005$ nm, a plate-shaped morphology and a Bain orientation relationship with the iron matrix. Their equilibrium composition (in atomic percentage) is reached after 38 h at 600°C and is the following: 76% Al, 16% Cr and 8% Mn for the (Al,Cr,Mn)N precipitates and 79% Al and 21% Cr for the (Al,Cr)N precipitates. These percentages do not take into account the proportion of nitrogen, which was not quantified.

3. From the experimental results obtained, a mechanism of formation of these nitrides was suggested. The initial precipitates formed in the early stages of annealing are probably of CrN or (Cr,Mn)N type. Indeed, the formation of cubic CrN platelets in steels is known to be easy, while that of AlN is more difficult. During a prolonged annealing, these initial precipitates serve as nucleation sites for the final precipitates and enrich in aluminium and nitrogen, to give finally cubic (Al,Cr)N and (Al,Cr,Mn)N particles. As a consequence, it is possible to precipitate all the nitrogen present in solid solution in the investigated steel, in spite of its sub-stoichiometry in aluminium.

4. Other types of steels (aluminum-killed steels, steels with different Al/Cr atomic ratios ....) will be investigated in further studies, in order to establish if the preceding results can be generalised to other systems.

Acknowledgements

The authors wish to thank the metallurgical research team of the "Laboratoire d'Etudes et de Développement des Produits Plats" (LEDEPP) of USINOR-Recherche Développement (Florange) for supplying the material.

References

1. R. H. GOODENOW, *Trans. Met. Soc. AIME* **59** (1966) 804.
2. P. N. RICHARD, *J. Australian Inst. Metals* **12** (1967) 2.
3. J. T. MICHALAK and R.D. SCHOONE, *Trans. Met. Soc. AIME* **242** (1968) 1149.
4. Y. MEYZAUD, B. MICHANT and P. PARNIÈRE, in " Texture and the Properties of Materials," edited by G. J. DAVIES *et al.* (The Metals Society, London, 1976) p. 255.
5. W. B. HUTCHINSON, *Int. Met. Rev.* **29**(1) (1984) 25.
6. R. C. HUDD, *Met. Mater.* **3**(2) (1987) 71.
7. J. MERLIN, N. LAVAIRE, M. ROCHER and M. BOUZEKRI, *Revue de Métallurgie*, Novembre 1999, 1413.
8. M. H. BIGLARI, C. M. BRAKMAN, M. A. J. SOMERS, W. J. SLOOF and E. J. MITTEMEIJER, *Z. Mettallkde* **84** (1993) 124.
9. M. F. ASHBY and L. M. BROWN, *Phil. Mag.* **8** (1963) 1083.
10. E. C. BAIN, *Trans AIME* **70** (1924) 25.
11. M. H. BIGLARI, C. M. BRAKMAN and E. J. MITTEMEIJER, *Phil. Mag.* **A72** (1995) 1281.
12. F. WEVER, K. KOCH, C. ILSCHNER-GENCH and H. ROHDE, *Forsh. Wirts. Nordrhein-Westfalen* **409** (1957) 1.
13. E. T. TUKDOGAN and S. IGNATOWICZ, *J. Iron Steel Inst.* **188** (1958) 242.
14. M. POPE, P. GRIEVESON and K. H. JACK, *Scan. J. Metall* **2** (1973) 29.
15. D. H. KIRKWOOD, O. E. ATASOY and S. R. KEOWN, *Metal Sci.* **8** (1974) 49.
16. D. H. JACK, *Acta Metall.* **24** (1976) 137.
17. H. H. PODGURSKI and F. N. DAVIS, *ibid.* **29** (1981) 1.
18. D. S. RICKERBY, S. HENDERSON, A. HENDRY and K. H. JACK, *ibid.* **34** (1986) 1687.

19. P. M. HEKKER, H. C. F. ROZENDAAL and E. J. MITTEMEIJER, *J. Mater. Sci* **20** (1985) 719.
20. J. N. LOCQUET, R. SOTO, L. BARRALLIER and A. CHARAÏ, *Microsc. Microanal. Microstruct.* **8** (1997) 335.
21. F. G. WILSON and T. GLADMAN, *International Materials Reviews* **33** (1988) 221.
22. M. H. BIGLARI, C. M. BRAKMAN, E. J. MITTEMEIJER and S. VAN DER ZWAAG, *Metall. Mater. Trans.* **A26** (1995) 765.
23. *Idem., Phil. Mag.* **A72** (1995) 931.
24. S. HANAI, N. TAKEMOTO and Y. MIZUYAMA, *Trans. ISIJ* **11** (1971) 24.
25. R. OGAWA, T. FUKUTSUKA and Y. YGAI, *ibid.* **12** (1972) 291.
26. H. S. CHOI, C. M. LEE and J. CHOI, *J. Korean Inst. Metals* **16** (1978) 485.

Received 30 November 1999
and accepted 16 October 2000